Journal of Solid State Chemistry **147,** 38–44 (1999)
Article ID jssc.1999.8156, available online at http://www.idealibrary.com on

Molecular Intercalation of Ammonia into Zirconium Disulfide

Lori A. Brown and William S. Glaunsinger[1]

Department of Chemistry and Biochemistry, Arizona State University, Tempe, Arizona 85287-1604

and

Michael J. McKelvy

Center for Solid State Science, Arizona State University, Tempe, Arizona 85287-1704

Received October 5, 1998; in revised form December 24, 1998; accepted December 30, 1998

The intercalation and deintercalation of NH_3 into ZrS_2 has been investigated by evolved gas analysis, thermogravimetric analysis, differential scanning calorimetry, vapor pressure measurements, SQID magnetometry, and X-ray powder diffraction. Ammonia intercalation of ZrS_2, in contrast to other transition metal disulfides (TS_2), is predominately a molecular insertion reaction. Only a small amount of NH_4^+ ($\leq 1\%$) is present in the intercalate, which may be required for intercalation to occur. The small degree of charge transfer can be understood qualitatively within the rigid-band model. The equilibrium intercalate, $(NH_3)_{0.92}ZrS_2$, can be indexed to a 3R, stage-1 structure having an occupied layer expansion (3.17 Å) in good agreement with other NH_3–TS_2 intercalation compounds. The guest–guest and guest–host interactions that stabilize the intercalate apparently involve $H_2N\text{–}H \cdots NH_3$ and $H_2N\text{–}H \cdots S$ hydrogen bonding, respectively. Based on this study, ammoniated ZrS_2 offers an excellent model system for probing the structure and properties of molecular guest species in lamellar materials.

INTRODUCTION

Early investigations of the intercalation of organic Lewis bases into transition metal dichalcogenide (TMD) hosts were thought to proceed by a molecular mechanism (1), with guest–host charge transfer arising from covalent overlap of molecular orbitals. More recently, redox chemistry has been found to be widely applicable to these systems. Redox-rearrangement reactions were discovered in these materials in 1977, when Schöllhorn and Zagefka proposed the co-intercalation of NH_4^+ ions during intercalation of NH_3 into $2H\text{–}TaS_2^2$ and reported the composition of the product as $(NH_4^+)_{y'}(NH_3)_{y''}TaS_2^{y'-}$, where $y' \cong 0.1$. Since then, several investigations have shown definitely that redox reactions are associated with intercalation of Lewis bases into TMDs (3–6).

The term redox-rearrangement is used because reactant molecules are structurally modified to form ionic species via redox reactions, which co-intercalate during intercalation. The most thoroughly characterized redox-rearrangement reaction is the NH_3 intercalation of lamellar TS_2 hosts, where T = Ti, Nb, and Ta (4–7). The intercalation mechanism can be represented by the following reaction sequence:

$$(y'/3)NH_3 \rightarrow (y'/6)N_2 + y'H^+ + y'e^-, \qquad [1]$$

$$y'H^+ + y'NH_3 \rightarrow y'NH_4^+, \qquad [2]$$

$$y'e^- + TS_2 \rightarrow TS_2^{y'-}. \qquad [3]$$

Such redox-rearrangement intercalation compounds are best described by the ionic formula $(NH_4^+)_{y'}(NH_3)_{y''}TS_2^{y''-}$, where T = Ti, Ta, Nb and $y' = 0.23 \pm 0.02$ for TiS_2 and NbS_2, and $y' = 0.08$ for TaS_2 (4–7). Thermal deintercalation of these metallic compounds typically produces NH_3 at lower temperatures and both NH_3 and H_2 at higher temperatures from the deintercalation/decomposition of NH_4^+.

A notable exception to the general redox-rearrangement mechanism is the simple molecular intercalation of hydrazine into semimetallic $TiSe_2$ (0.1 eV sulfur p- and metal d-band overlap) (8, 9). Evidence for molecular intercalation includes the absence of N_2 or H_2 evolution during intercalation or deintercalation of N_2H_4, respectively. The driving force for N_2H_4 intercalation is apparently strong guest-to-host charge transfer that has been estimated to be 0.34 mol e^-/mol $TiSe_2$ for $(N_2H_4)_{0.6}TiSe_2$ from conductivity measurements (10). The mechanism of charge transfer appears to be covalent overlap of the N_2H_4 lone pair(s) with

---

[1] To whom correspondence should be addressed.

0022-4596/99 $30.00

available host-layer states, as originally proposed for ammoniated TaS_2 (11). Similar results have been observed for N_2H_4 intercalation of $1T$–TaS_2 (9). Molecular N_2H_4 intercalation has also been proposed for TiS_2 and ZrS_2 (9, 10). However, there is evidence of host-layer attack in these systems, so they are more properly considered to be pseudo-intercalation compounds (12).

ZrS_2 is known to intercalate ammonia, but the guest species have not been characterized to date (13). This reaction is ideal for the study of charge transfer because ZrS_2 is isostructural and has a similar band structure to TiS_2. The most significant difference is that ZrS_2 is a large band-gap (1.5 eV) semiconductor, whereas TiS_2 has been described as a narrow-gap (0.2–0.3 eV) extrinsic semiconductor (14–16). This difference was anticipated to contribute to a higher chemical potential of the ZrS_2 host compared to TiS_2, which should reduce charge transfer during intercalation. However, it is unclear to what extent the charge transfer would be reduced for ZrS_2 compared to TiS_2 because there are no direct comparisons of the energy levels for these hosts in the literature. This provides the motivation for this study of extent of charge transfer for the NH_3–ZrS_2 intercalation system.

EXPERIMENTAL

Host Synthesis and Characterization

Highly stoichiometric zirconium disulfide, $Zr_{1,000+0.001}S_2$, was prepared from the elements using Marz-grade Zr wire purchased from Materials Research Corp. The main impurity noted in the certificate of conformance provided by the manufacturer was 20 ppm Fe. Sulfur pieces (99.999%), purchased from Aldrich, were used instead of powder, as they facilitate more quantitative transfer of the sulfur to the reaction ampule. This is important for the synthesis of ZrS_2, as stoichiometric amounts of the elements were reacted in 1 g lots, with only a slight S excess (1–3 mg), to avoid formation of ZrS_3 (17).

The Zr wire was folded into a bundle and cleaned by sonication in trichloroethylene (AR grade; evaporation residue $\leq 0.0001\%$) three times to remove any oils from processing. Then it was rinsed three times in 25 mL toluene (AR grade; evaporation residue $\leq 0.00001\%$). The clean wire was placed into a previously cleaned alumina boat and inserted into a quartz ampule. The alumina provides a physical barrier between the Zr and the quartz to prevent the formation of zirconia at high temperatures (18). The boat was previously sonicated in 4% EDTA solution for 15 min and then rinsed with doubly distilled water 25 times, followed by baking at 1000°C overnight to remove volatile contaminants. Ampules containing S and Zr in alumina boats were connected to a stopcock assembly, evacuated to 10^{-5} Torr on a vacuum line, and then flame-sealed.

Several sealed quartz ampules were inserted into a programmable three-zone Lindberg furnace. The quartz ampules were equipped with external legs to avoid rolling of ampules during insertion into the furnace. The furnace was programmed to slowly heat the samples at 0.1°C/min from ambient temperature to 500°C, where they were held for 48 h. Then the temperature was raised at 0.1°C/min to 800°C and held for another 48 h. The ampules were quickly removed and quenched in a water bath to avoid ZrS_3 formation (17). The yellow ghost of trace excess sulfur was sublimed away from the product, with the product end of the ampule at 320°C and the other end at ambient temperature.

All samples were manipulated in a Vacuum Atmospheres (Model MO-40-1H, <1 ppm H_2O and O_2) He-filled glovebox, because they react with oxygen and water in air (16). The ampules were scored and wrapped with Parafilm to prevent quartz particles from falling into the sample and then snapped open. Four ampules of the reddish-brown material were pulverized in an agate mortar to a fine powder and placed in a single new quartz ampule. The ampule was then evacuated to 10^{-5} Torr, flame-sealed, and annealed at 800°C for 5 days. Again, ampules removed from the furnace were water-quenched to avoid any ZrS_3 formation (17).

Thermogravimetric analysis (TGA) was performed using a Perkin–Elmer TGS-2 system having 0.1 μg sensitivity and 0.01% weight resolution. The stoichiometry of ZrS_2 samples was determined by TGA of their oxidation to ZrO_2 in pure oxygen (99.995%) at 900°C.

Approximately 50 mg of ZrS_2 was placed in a platinum pan that was loaded onto the TGA balance. The furnace/shield was raised around the sample at 110°C, with an O_2 flow rate of 12 cm^3/min. The subsequent heating rate was 2°C/min. The ZrS_2 host is stable up to 185°C, as evidenced by constant sample weight over this temperature range. The final wt% of ZrO_2 was $79.42 \pm 0.03\%$ of the initial sample weight, which corresponds to a stoichiometry of $Zr_{1.003\pm0.001}S_2$. Analysis of the residual sulfur in ZrO_2 by Guelph Chemical Laboratories Ltd. gave a final stoichiometry of $Zr_{1.000\pm0.001}S_2$.

The host and thermally deintercalated host were characterized by X-ray powder diffraction (XPD) to probe the reversibility of intercalation. Samples for XPD were loaded into 0.3 mm Pyrex capillaries in the glovebox. XPD patterns were recorded at ambient temperature using Ni-filtered Cu$K\alpha$ radiation and a Debye–Scherrer camera previously calibrated with NBS SRM 640 silicon. Lattice parameters were determined by least-squares refinement of the data.

Ammonia Intercalation and Characterization

The host was weighed to the nearest 0.1 mg inside the glovebox and loaded into one leg of a pyrex H-tube with a break seal and stopcock assembly. The reaction vessel was evacuated to 10^{-5} Torr on a high-vacuum line. Ammonia, previously dried over Na, was condensed using liquid nitrogen into the opposite leg. The vessel was flame-sealed and placed in a styrofoam container, and the NH_3 allowed to come to ambient temperature. This was a routine precaution to verify a good seal. The liquid NH_3 was then slowly poured onto the host. Intercalation was marked by flocculation of the particles and expansion of a cylindrical column of the material.

The intercalate was isolated from the excess NH_3 by slowly pouring the liquid NH_3 back into the second leg, which was equipped with a break seal. The intercalate was rinsed three times by distilling the excess NH_3 onto the intercalate and decanting it into the opposite leg. The NH_3 leg was placed slowly in a liquid-nitrogen bath to reduce the pressure inside the vessel. As the last of the NH_3 solidified, the leg containing the intercalate was immersed in a dry ice–ethanol bath to minimize deintercalation of volatile guest species. The intercalate was isolated from the NH_3 leg of the H-tube by forming a flame seal between the two legs. Approximately a 50% expansion in the ZrS_2 column height was observed after several weeks of reaction.

The contents of the NH_3 leg were analyzed by evolved-gas analysis (EGA). The vessel was connected to a residual-gas analysis (RGA) system and chilled to liquid-nitrogen temperature for analysis of noncondensable gases. After a period of an hour or greater, the seal was broken and the contents were released into the vacuum line. The pressure was measured using a Baratron gauge, and the mass spectrum was collected using a Hiden Residual Gas Analyzer.

The stoichiometry and deintercalation behavior of the volatile components of the intercalate were determined by TGA (19). Samples were hermetically sealed in aluminum pans in the glovebox, weighed to the nearest 0.1 mg, and transferred to the instrument using glass weighing bottles placed into a tightly sealed Ball jar. The TGA was encased in a homemade glovebox, which was flushed with N_2 before the sample was transferred to the TGA balance. The sample pans were pierced immediately prior to analysis to allow any gases to escape. The TGA carrier gas was ultrapure (99.999%) argon, which had been passed through a titanium metal purifier at 925°C. The heating rate was 2°C/min.

The guest species were characterized by vapor pressure measurements (VPM) and RGA of the gases thermally deintercalated from the material using the experimental setup for EGA.

Differential scanning calorimetry (DSC) measurements were performed using a Perkin–Elmer DSC-4. The system was calibrated using the melting transition of indium. Samples were hermetically sealed in aluminum pans and weighed in the glovebox to the nearest 0.1mg. They were then transferred to a nitrogen-filled glovebag encasing the DSC head. The pans were pierced immediately prior to analysis to permit escape of volatile species. A heating rate of 5°C/min and sample weights of 3–4 mg were used.

Since ammoniated-ZrS_2 compounds were observed to lose NH_3 under ambient conditions, the fully intercalated material was structurally analyzed using loaded XPD capillaries sealed under 300 Torr of NH_3. XPD patterns were recorded at ambient temperature using Ni-filtered Cu$K\alpha$ radiation and a Debye–Scherrer camera previously calibrated with NBS SRM 640 silicon. The lattice parameters were determined by a least-squares refinement of the data.

The magnetic susceptibility of the compounds was measured from 1.6 to 400 K in magnetic fields up to 50.00 kOe using a SHE (BTI) VTS 905 SQUID magnetometer. Large samples (100–150 mg) were loaded into Delrin buckets inside the glovebox. Silicone grease (Dow Corning) was applied to the threaded top to seal the bucket during sample transfer to the magnetometer.

RESULTS AND DISCUSSION

Characterization of the Intercalation Compound

Visual observations reveal important characteristics of the intercalation of NH_3 into TS_2 hosts. The most obvious changes that occur during intercalation of NH_3 into TiS_2 are (i) a continuous stream of bubbles in the excess liquid NH_3 due to N_2 evolution, (ii) a color change of the excess liquid NH_3 above the sample due to formation of a polysulfide solution, (iii) 50% expansion in a cylindrical column of material, and (iv) a darkening of the material as electrons are transferred to the host. In contrast, the NH_3 solution above ZrS_2 was colorless after several months, and the product maintains the reddish-brown color of the pristine host. In addition, there was no visible residue left in the reaction vessel upon evaporation of the excess liquid NH_3, which would have indicated polysulfide formation. Several hours after the start of the reaction, the only indications of reaction were flocculation of the particles accompanied by swelling of the material. Reactions times of 3–4 weeks were required for a 50% expansion of the original column height.

A typical TGA curve of the intercalate shown in Fig. 1a displays a one-step weight loss that is characteristic of a single chemical species being evolved from the sample. For comparison, the two-step TGA curve for sequential deintercalation of NH_3 and NH_4^+ from $(NH_4^+)_{0.22}(NH_3)_{0.37}TiS_2^{0.22-}$ is shown in Fig. 1b (4). The second step in Fig. 1b represents the deintercalation of NH_4^+ quantitatively above 150°C as 67% NH_3 and 33% H_2. Essentially all of the NH_3 is deintercalated from ZrS_2 by 180°C, followed by a slight tail in the TGA curve that was found to be independent of intercalate composition. Extended heating to 230°C was required for complete deintercalation. The sample stoichiometry was found to be dependent on sample history because of the volatility of intercalated NH_3. Therefore, samples were stored in sealed ampules or sample containers prior

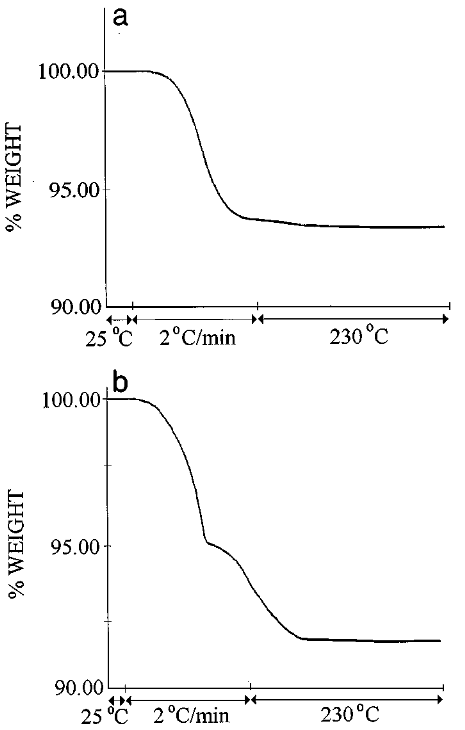

FIG. 1. TGA curves of the deintercalation of nominally $(NH_3)_{0.66}ZrS_2$ and $(NH_4^+)_{0.23}(NH_3)_{0.39}TiS_2^{0.22-}$ (19). The weight loss in (a) and the first step in (b) are associated with the removal of molecular NH_3 species at low temperatures (<175 and <150°C, respectively), where the intercalate NH_3 composition is dependent upon sample history. The second step in (b) corresponds to the deintercalation of NH_4^+ as a 1:2 molar ratio of $H_2:NH_3$. Note the slight weight loss above ≈175°C in (a) corresponds to <1% NH_4^+ deintercalation.

to all experiments, and the precise NH_3 composition was determined prior to each experiment (19).

The equilibrium stoichiometry of the intercalate was determined by VPM at 300 Torr NH_3 pressure. EGA upon deintercalation of ammoniated ZrS_2 was performed to identify the gaseous deintercalation products. During deintercalation, all of the gas evolved by 180°C was condensable in a liquid-nitrogen trap. The sample was heated to 300°C to ensure complete deintercalation. The condensable gas was determined by residual gas analysis to be pure NH_3. The composition of the intercalation compound was calculated to be $(NH_3)_{0.92}ZrS_2$. The only noncondensable gas evolved above 180°C was identified as H_2, which corresponds to a host ammonium content of only $y' = 0.012 \pm 0.006$. Therefore, very little NH_4^+ has co-intercalated in ZrS_2, in contrast to the ammonia intercalation behavior of other TS_2 hosts (3–6).

The XPD pattern of $(NH_3)_{0.25}ZrS_2$ indicated a mixed-phase material. Reflections from unreacted host were observed in addition to those of another phase. The latter phase could not be indexed due to the paucity and broadness of the lines. In contrast, all reflections from the XPD pattern for $(NH_3)_{0.92}ZrS_2$ obtained under 300 Torr NH_3 were indexed as a stage 1 (i.e., every host gallery is occupied by NH_3), 3R compound, with $a = 3.664(3)$ Å and $c = 26.95(7)$ Å. The observed pattern is in reasonable agreement with that expected for the 3R structure, where the ZrS_2 layers have shifted during intercalation to provide trigonal prismatic interlayer guest sites (12, 13). (An introduction to the polytypes of TX_2 materials and the related phase transitions during intercalation can be found in Ref. (20).) Trigonal prismatic coordination of sulfur about NH_3 allows hydrogen bonding to neighboring NH_3 molecules. This is consistent with the C_3 axis of NH_3 being parallel to the host layers, as found in previous studies of NH_3 in TiS_2 and TaS_2 (11, 21). The occupied-layer expansion (OLE) of 3.17 Å for $(NH_3)_{0.92}ZrS_2$ is also in good agreement with the range of OLEs observed for ammoniated TiS_2 and NbS_2 with different ammonia compositions (3.01–3.21 Å) (5, 19).

The stoichiometry of the deintercalated host $(Zr_{1.000 \pm 0.001}S_2)$ was in excellent agreement with the pristine host. Good registry of the layers was indicated by the sharpness of the XPD pattern, where $a = 3.661(3)$ Å and $c = 5.823(10)$ Å. The observed d spacings are in good agreement with those calculated from the lattice parameters (13). These results indicate that the intercalation process is reversible to a good approximation.

Guest-to-Host Charge Transfer

EGA was performed to characterize the contents of the reaction vessel that contained the colorless ammoniacal intercalation solution. First, gases that were condensable at liquid-nitrogen temperature were solidified for the purpose of quantifying any noncondensable gases present. It was found for six individual syntheses that only 1.3×10^{-3} mol N_2 per mol ZrS_2 was evolved during intercalation, corresponding to an ionic formula of $(NH_4^+)_{0.008}(NH_3)_{y''}ZrS_2$, compared to 4.2×10^{-2} mol N_2 per mol TiS_2, where $y' = 0.25$ (4). This composition is in good agreement with EGA of the H_2 evolved during thermal deintercalation of the ZrS_2 intercalate. It is clear from the relatively small amount of NH_4^+ relative to NH_3 (<1%) that molecular guest species dominate the chemical and physical properties of this intercalate. Consequently, it is best classified as a molecular intercalation compound, $(NH_3)_yZrS_2$. However, trace amounts of NH_4^+ indicate a small degree of charge transfer, accompanied by redox-rearrangement chemistry that may be necessary to initiate intercalation.

Charge transfer between adsorbate guest species and the host layers has been envisioned as the source for loosening the external-most gallery at the beginning of the intercalation process (2). In particular, a preintercalation state has been discovered by Wang *et al.* for NH_3 insertion into TiS_2 that is defined by pressure-independent charge transfer from adsorbed NH_3 on the basal plane (22). After intercalation, they argue that summation of the charge transfer to the external layer from adsorbed NH_3 (0.07 e^- per TiS_2 unit) and the internal guest layer (0.12 e^- per TiS_2 unit) does not account for the total observed charge transfer (0.24 e^- per TiS_2 unit) in the bulk intercalate. They propose that the difference (0.05 e^- per TiS_2 unit) results from diffusion of protons to the adsorbate layer to form ammonium ions. A similar intercalation process can be envisioned, albeit with much lower NH_4^+ intercalant concentrations, for ammoniated ZrS_2.

The guest-to-host charge transfer for ammoniated TiS_2 and NbS_2 corresponds to one mol e^-/mol NH_4^+, as determined from magnetic susceptibility (χ) measurements for electrically conductive $(NH_4^+)_{0.19}(NH_3)_{0.27}TiS_2^{0.19-}$ and $(NH_4^+)_{0.23}(NH_3)_{0.31}NbS_2^{0.23-}$ (3, 5). The contribution from the intercalated NH_3 species in the above compounds was found to be negligible. ZrS_2 displays a very small temperature-independent diamagnetic susceptibility ($\chi = -16 \times 10^{-6}$ emu/mol ZrS_2) characteristic of an electrical insulator. There was no increase in χ for $(NH_3)_{0.48}ZrS_2$ relative to pristine ZrS_2 within experimental error ($\pm 4 \times 10^{-6}$ emu/mol ZrS_2). Since the band structures of TiS_2 and ZrS_2 are similar, as discussed in the next section, guest-to-host charge transfer for ammoniated ZrS_2 is estimated to be below 0.02 mol e^-/mol ZrS_2, in good agreement with ammoniated ZrS_2 intercalation and deintercalation EGA.

It is instructive to compare the total NH_3 content ($y = y' + y''$) for TiS_2 and ZrS_2 as a function of reaction time with liquid NH_3. For example, $y = 0.40$ in TiS_2 approximately 4 h after pouring liquid NH_3 onto the host (4), whereas a period of 2 weeks is required for ZrS_2 to achieve this composition. This would suggest that molecular intercalation occurs at a much slower rate than redox-rearrangement intercalation. However, intercalation of molecular hydrazine (N_2H_4) in TX_2 hosts is a spontaneous reaction (8). The enhanced reactivity is thought to be related to strong preintercalation and intercalation charge transfer (19, 12, 22). This is consistent with strong molecular charge transfer associated with bulk hydrazine intercalates, where the charge transfer is 0.34 e^-/mol $TiSe_2$ for $(N_2H_4)_{0.6}TiSe_2$ (10). Therefore, intercalation reactivity appears to be strongly associated with the degree of guest-to-host charge transfer.

The extent of charge transfer associated with NH_3 intercalation into TS_2 hosts is summarized in Table 1 and can be understood, at least qualitatively, within the rigid-band model (20, 23, 24). In this model, the guest electrons are transferred to the unperturbed conduction band of the host. For example, in the compound $(NH_4^+)_{0.23}(NH_3)_{0.22}TiS_2^{0.23-}$, the charge transfer is 0.23 ± 0.02 mol e^-/mol TiS_2, as shown in Fig. 2 (4, 26). Since charge transfer was found to be substantially lower in ZrS_2, it follows that the conduction band is higher in energy relative to TiS_2. Support for a higher conduction band energy for MoS_2 comes from the lack of reaction of NH_3 with MoS_2. Highly stoichiometric MoS_2 (< 0.1 mol% excess Mo) does not directly intercalate NH_3 over a wide range of temperature and pressure (12). The band diagram in Fig. 2 illustrates the filled transition metal d_{z^2} band in MoS_2 (20). In order for charge transfer to occur, the electrons must be transferred to the next available states in the upper d band. These states must, therefore, be relatively high in energy due to the large band gap in MoS_2, leaving NH_3-to-MoS_2 charge transfer as thermodynamically unfavorable, and intercalation does not occur.

TABLE 1

Degree of Charge Transfer in Ammoniated TS_2 Compounds

Host	y'[a]
TiS_2	0.23[b]
NbS_2	0.23[c]
2H–TaS_2	0.08[d]
ZrS_2	0.008
MoS_2	No reaction[e]

[a] y' represents mol NH_4^+ per mol of host.
[b] Reference (4).
[c] Reference (5).
[d] References (2) and (7).
[e] References (12) and (23).

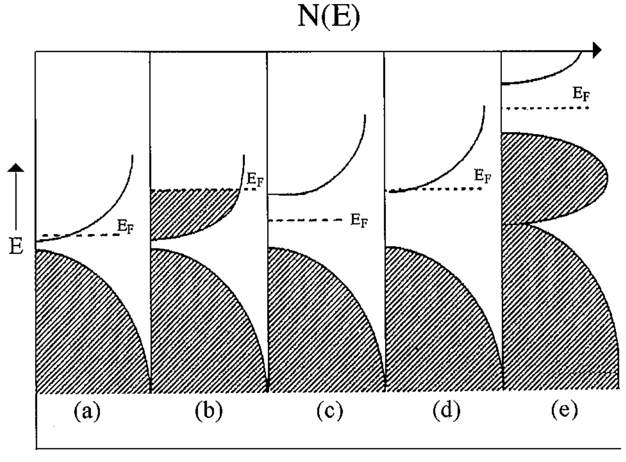

FIG. 2. Simplified band diagrams for TiS_2 (a), $(NH_4^+)_{0.23}(NH_3)_{0.22}TiS_2^{0.23-}$ (b), ZrS_2 (c), $(NH_4^+)_{0.008}(NH_3)_{0.99}ZrS_2^{0.008-}$ (d), and 2H–MoS_2 (e), where the dashed lines indicate the position of the Fermi level (E_F) (23, 24). The lower valence bands comprised mainly of sulfur p orbitals are completely filled, as indicated by the shading. The electrons are transferred to d_{z^2} orbitals that make up the conduction bands of TiS_2 and ZrS_2 during NH_3 intercalation. Note that TiS_2 is actually an extrinsic semiconductor instead of an intrinsic semiconductor (14–16). In MoS_2, charge transfer from NH_3 is not favored because the d_{z^2} band is completely filled (24).

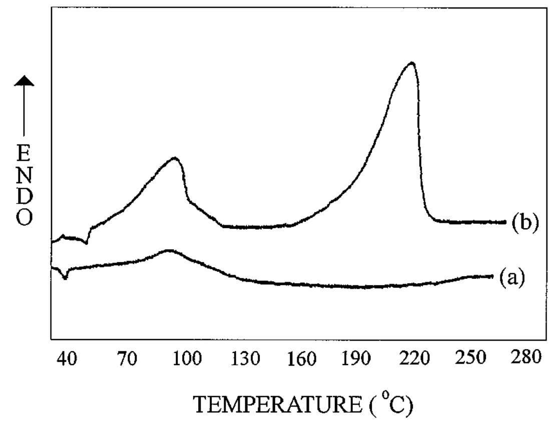

FIG. 3. (a) A typical DSC curve for the thermal deintercalation of $(NH_3)_{0.48}(ZrS_2)$ displays a single endothermic event, where $\Delta H_{NH_3} =$ 5 kcal/mol NH_3. The onset temperature (50°C) and broadness of this event are in good agreement with TGA results. In contrast, the DSC curve for $(NH_4^+)_{0.22}(NH_3)_{0.23}TiS_2^{0.22-}$ (b) shows two peaks that represent sequential deintercalation of NH_3 and NH_4^+ (19). The initial small decrease prior to the endothermic peaks is due to instrumental startup.

Guest–Host and Guest–Guest Interactions

The DSC curve for the deintercalation of $(NH_3)_{0.48}ZrS_2$, shown in Fig. 3a, displays only one endothermic event, as expected for deintercalation of NH_3 alone. The very low level of NH_4^+ deintercalation is below the resolution of the DSC. The onset temperature of 50°C is in good agreement with the deintercalation of NH_3 from ZrS_2 found in TGA experiments. The enthalpy of deintercalation estimated from the area under the curve is 5 kcal/mol NH_3 (± 1 kcal). It is instructive to compare this value to those of related ammoniated intercalates. A summary of the deintercalation enthalpies of NH_3 in ammoniated ZrS_2, NbS_2, 2H–TaS_2, and TiS_2 is given in Table 2. The smaller value for the enthalpy of deintercalation of NH_3 from ammoniated ZrS_2 indicates that it is more weakly bound than NH_3 in other TS_2 hosts. The ion–dipole/ion–induced dipole interactions between NH_4^+ and NH_3 present in the other intercalates apparently contributes to their higher ammonia deintercalation enthalpies.

Since there is essentially only one guest species, NH_3, present in ammoniated ZrS_2, there are only two primary interactions that need to be addressed: (i) NH_3–NH_3 and (ii) NH_3–ZrS_2. Another factor that contributes to the NH_3 deintercalation enthalpy is the host-layer expansion energy associated with the collapse of the layers to the original host separation. This contribution has been estimated at 1–2 kcal/mol NH_3 (25). The NH_3–NH_3 interactions can be compared to hydrogen bonding in bulk NH_3 (2.30 kcal/mol NH_3) (26). Six hydrogen bonds are formed in solid NH_3, where three act as donors and three act as acceptors. The number of NH_3–NH_3 hydrogen bonds possible for a parallel monolayer of NH_3 in ZrS_2 is reduced to a maximum of two per NH_3 (one H acceptor and one H donor), with an estimated associated energy of less than 1 kcal/mol NH_3. It follows that the stability of the intercalate is most dependent on NH_3–ZrS_2 interactions.

TABLE 2
Deintercalation Enthalpies for Ammoniated *TS_2*

Compound	ΔH_{NH_3} (kcal/mol NH_3)
$(NH_3)_{0.48}ZrS_2$	5
$(NH_4^+)_{0.23}(NH_3)_{0.34}NbS_2^{0.23-}$	7.6[a]
$(NH_4^+)_{0.08}(NH_3)_{0.85}TaS_2^{0.08-}$	8[b]
$(NH_4^+)_{0.22}(NH_3)_{0.23}TiS_2^{0.22-}$	10.5[c]

[a] Reference (5).
[b] References (19) and (25).
[c] Reference (19).

There are two possible types of NH_3–ZrS_2 interactions: (i) interaction of the nitrogen lone pair with the host and (ii) hydrogen bonding of the NH_3 molecule to the host-layer sulfur atoms. The first type of interaction requires perpendicular orientation of the C_3 axis of NH_3 relative to the host layers. This is the optimum orientation for guest-to-guest orbital overlap and concomitant charge transfer. However, the presence of very little change transfer in ammoniated ZrS_2 suggests any energetic advantage of the perpendicular orientation must be small and come at the expense of eliminating NH_3 hydrogen bonding to neighboring NH_3 molecules. In addition, the pseudo-C_3 axis of NH_3 in TiS_2 and TaS_2 hosts is known to be parallel to the host layers from NPD (21, 26) and NMR (11) studies, which minimizes NH_3 electron transfer to the lost layers (12, 26).

Hydrogen bonding of NH_3 to sulfur in TS_2 hosts has been shown to be a significant guest-host interaction in $(ND_4^+)_{0.22}(ND_3)_{0.24}TiS_2^{0.22-}$, where two of the deuterium atoms are oriented for maximum hydrogen bonding to the sulfur layers and the third lies on the interlayer midplane (26). The existence of hydrogen bonding for the former deuterium atoms is further evidenced by $D \cdots S$ distances of less than 2.7 Å, which are significantly less than the D–S van der Waals contact distance of 3.1 Å (26). The existence of ammonia hydrogen bonding for these intercalates is underscored by the very similar activation energies for ammonia C_3 axis rotation for $(NH_4^+)_{0.22}(NH_3)_{0.37}TiS_2^{0.22-}$ (2.41 ± 0.02 kcal/mol NH_3) and solid NH_3 (2.30 kcal/mol NH_3) (26, 27). Hence, it appears that the hydrogen-bonding interactions in these intercalates are comparable to those in solid NH_3.

An often-neglected contribution to the strength of a hydrogen bond is the polarizability of the electronegative atoms (28, 29). Sulfur, being more polarizable than nitrogen, contributes more electron density to the hydrogen bond than nitrogen. Therefore, hydrogen bonding of the NH_3 to sulfur, albeit a relatively weak interaction, apparently makes a significant contribution (≥ 2 kcal/mol NH_3) to the measured deintercalation enthalpy (5 kcal/mol NH_3).

CONCLUSIONS

The results of this study indicate that ammoniated ZrS_2, unlike other ammoniated TS_2 hosts where redox reactions predominate, can be best described as a molecular intercalation compound. The small amount of NH_4^+ relative to NH_3 ($<1\%$) may be required for intercalation to occur. This intercalation is apparently stabilized by hydrogen-bonding interactions of the type $H_2N\text{–}H \cdots NH_3$ and $H_2N\text{–}H \cdots S$. This investigation has demonstrated that $NH_3\text{–}ZrS_2$ intercalates, as well as probably other amine–ZrS_2 intercalates, provide unique model systems for practicing molecular intercalation chemistry, just as Hg_xTiS_2 has proven to be an intriguing system for practicing covalent electron-exchange intercalation chemistry in the essential absense of charge transfer (30).

ACKNOWLEDGMENTS

We acknowledge Jean Rouxel and John Goodenough for stimulating discussions of the properties of transition metal dichalcogenides. We also acknowledge the National Science Foundation for support through Grant DMR 91-06792 and the ASU Center for Solid State Science for the use of the Materials Facility in the Goldwater Materials Science Laboratories.

REFERENCES

1. R. B. Somoano, V. Hadek, and A. Rembaum, *J. Chem. Phys.* **58,** 697 (1973).
2. R. Schöllhorn and H. D. Zagefka, *Angew. Chem. Int. Ed. Engl.* **16,** 199 (1977).
3. L. Bernard, M. J. McKelvy, W. S. Glaunsinger, and P. Colombet, *Solid State Ionics* **15,** 301 (1985).
4. M. J. McKelvy and W. S. Glaunsinger, *Solid State Ionics* **25,** 287 (1987).
5. J. M. Dunn and W. S. Glaunsinger, *Solid State Ionics* **27,** 285 (1988).
6. R. Schöllhorn, H. D. Zagefka, and T. Butz, *Mater. Res. Bull.* **14,** 369 (1979).
7. L. A. Diebolt, The Synthesis, Characteristics, and Electron Microscopy of Intercalation Compounds of Tantalum Disulfide, Ph.D. Thesis, Arizona State University, 1995.
8. M. Sarma, A. R. Beal, S. Nulsen, and R. H. Friend, *J. Phys. C* **15,** 4367 (1982).
9. A. M. Ghoyareb, Charge Transfer in the Intercalation Complexes of Layered Compounds, Ph.D. Thesis, Cambridge University, Cambridge, England, 1985.
10. A. M. Ghorayeb and R. H. Friend, *J. Phys. C* **20,** 4181 (1987).
11. F. R. Gamble and B. G. Silbernagel, *J. Chem. Phys.* **63,** 2544 (1975).
12. M. J. McKelvy and W. S. Glaunsinger, *Annu. Rev. Phys. Chem.* **41,** 497 (1990).
13. J. Cousseau, L. Trichet, and J. Rouxel, *Bull. Soc. Chem. Fr.* 872 (1973).
14. H. W. Myron and A. J. Freeman, *Phys. Rev. B* **11,** 2087 (1975).
15. A. Zunger and A. J. Freeman, *Phys. Rev. B* **16,** 906 (1977).
16. M. J. McKelvy and W. S. Glaunsinger, *J. Solid State Chem.* **66,** 181 (1987).
17. C. R. Whitehouse, H. P. B. Rimmington, and A. A. Balchin, *Phys. Stat. Sol. A* **18,** 623 (1973).
18. R. Jellinek, *Acta Chem. Scand.* **16,** 791 (1962).
19. M. J. McKelvy and W. S. Glaunsinger, *J. Solid State Chem.* **67,** 142 (1987).
20. G. V. Subba Rao and M. W. Shafer, *in* "Intercalated Layered Materials" (F. Levy, Ed.), p. 99. D. Reidel, Dordrecht, 1979.
21. V. G. Young, Jr., M. J. McKelvy, W. S. Glaunsinger, and R. B. Von Dreele, *Chem. Mater.* **2,** 75 (1990).
22. C. Wang, M. J. McKelvy, and W. S. Glaunsinger, *J. Phys. Chem.* **100,** 19218 (1996).
23. J. A. Wilson and A. D. Yoffe, *Adv. Phys.* **18,** 193 (1969).
24. W. Y. Liang, "Physics and Chemistry of Electrons and Ions in Condensed Matter," p. 459. D. Reidel, Dordrecht, 1984.
25. M. Dines and R. Levy, *J. Phys. Chem.* **79,** 1979 (1975).
26. V. G. Young, Jr., M. J. McKelvey, W. S. Glaunsinger, and R. B. Von Dreele, *Solid State Ionics* **26,** 47 (1988).
27. G. W. O'Bannon, W. S. Glaunsinger, and R. F. Marzke, *Solid State Ionics* **26,** 15 (1988).
28. S. Lifson, A. T. Hagler, and P. Dauber,*J. Am. Chem. Soc.* **101,** 5111 (1979).
29. H. Umeyama and K. Morokima, *J. Am. Chem. Soc.* **99,** 1316 (1977).
30. E. W. Ong, M. J. McKelvy, G. Ouvrard, and W. S. Glaunsinger, *Chem. Mater.* **4,** 14 (1992).